Solitons Northeast of Tung-Sha Island During the ASIAEX Pilot Studies

Ying-Jang Yang, Tswen Yung Tang, M. H. Chang, Antony K. Liu, Ming-Kuang Hsu, and Steven R. Ramp

***Abstract*—In a recent study, satellite images have shown that internal solitons are active in the northern South China Sea (SCS). During the Asian Seas International Acoustic Experiment (ASIAEX) pilot studies, current profiler and thermistor chain moorings were deployed in the spring of 1999 and 2000 to investigate internal solitons northeast of Tung-Sha Island on the continental slope of the northern SCS. Most of the observed internal solitons were first baroclinic mode depression waves. The largest horizontal current velocity, vertical displacement, and temperature variation induced by the internal solitons were around 240 cm/s, 106 m, and 11 °C, respectively, while the estimated nonlinear phase speed was primarily westward at 152 ± 4 cm/s. The observed internal solitons could be categorized as four types. The first type is the incoming wave from deep water and can be described reasonably well with the KdV equation. The second and third types are in the transition zone before and close to the turning point (where the upper and lower layer depths are equal), respectively. These two types of solitons were generally near the wave-breaking stage. The fourth type of soliton is a second baroclinic mode and probably was locally generated. The time evolutions are asymmetric, especially at the middle depths. A temperature kink following the main pulse of the soliton is often seen. Higher order nonlinear and shallow topographic effects could be the primary cause for these features.The appearance/disappearance of internal solitons coincides mostly with spring/neap tide. The internal soliton is irregularly seen during the neap tide period and its amplitude is generally small. The time interval between two leading solitons is generally around 12 h. The first baroclinic mode of the semidiurnal tide has a larger amplitude than the diurnal tide and could redistribute its energy into the soliton.**

***Index Terms*—Internal wave, nonlinear wave, soliton, South China Sea (SCS).**

Manuscript received October 9, 2003; revised April 26, 2004. This work was supported by the National Science Council, Taiwan, R.O.C., under Grant NSC 90-2611-M-012-001-OP2 and Grant NSC 90-2611-E-012-001 awarded to Y.-J. Yang, Grant NSC 89-2611-M-002-027 awarded to T. Y. Tang, and Grant NSC 89-2611-M-019-014-OP2 awarded to M.-K. Hsu, and by the United States Office of Naval Research under Grant N00014-00-F-0165 awarded to A. K. Liu and Grant N00014-01-WR-20044 awarded to S. R. Ramp.

Y.-J. Yang is with the Department of Marine Science, Chinese Naval Academy, Kaohsiung 813, Taiwan, R.O.C.

T. Y. Tang and M. H. Chang are with the Institute of Oceanography, National Taiwan University, Taipei 106, Taiwan, R.O.C.

A. K. Liu is with the Goddard Space Flight Center, National Aeronautics and Space Administration, Greenbelt, MD 20771, USA.

M.-K. Hsu is with the Kuang Wu Institute of Technology, Taipei 112, Taiwan, R.O.C.

S. R. Ramp is with the Department of Oceanography, Naval Postgraduate School, Monterey, CA 93943 USA.

Digital Object Identifier 10.1109/JOE.2004.841424

I. Introduction

AN INTERNAL solitary wave is a localized internal gravity wave that occurs in a stratified fluid. It induces strong vertical motion, vertical shear of horizontal velocity, density perturbations, and probably nutrient pumping [1]. It also impacts the stability of oil platforms [2], the security of submarine navigation [3], and underwater acoustic propagation [4]–[7]. In 1834, Russell [8], [9] made the first observation of solitary waves. Boussinseq [10] and Korteweg and deVries [11] gave a theoretical description, hereafter referred to as KdV, which represented the extent of physical understanding of solitary waves up to that time. The solitary wave has a particle-like behavior. Zabusky and Kruskal [12] coined the word "soliton" to describe it.

Apel *et al.* [3] proposed two possible mechanisms for the generation of an internal soliton: 1) coupling of energy between tidal modes and 2) the release of a standing lee wave off the shelf break. In the former generation mechanism, energy from the barotropic tide is scattered into the internal modes within the tidal band at the shelf break. Here, the mode angle of the internal propagation characteristics coincides with the angle of the sloping bottom. The internal tides then scatter energy nonlinearly into the buoyancy band as they propagate shoreward. In the second mechanism, a strong barotropic tidal flow over a sill establishes a standing lee wave. At the onset of the flow reversal, typically occurring at slack tide, the lee wave travels upshelf as internal tides couple energy into the buoyancy band as soliton wave packets.

Assuming a two-layer ocean, Liu *et al.* [13] have discussed the propagation and transformation of the internal soliton from the deep ocean to shallow water. The internal soliton is a depression wave in the deep ocean. When it passes the turning point, where the thickness of upper and lower ocean water column are equal, the depression wave transforms into an elevation wave. The area of transformation is called a transition zone [14], [15]. During the transformation from a depression to an elevation wave, the soliton changes its shape gradually. In the transition zone, the coefficient of quadratic nonlinearity goes to zero in the typical KdV theory and the cubic or higher order nonlinear effect becomes important [14], [16]–[18]. When the internal soliton propagates from the deep ocean to the continental-slope region, the shoaling effect does not allow the soliton tail to return to its initial state and the mass is not conserved [14], [15], [19]. The higher order nonlinear effect of shoaling may generate the "kink" of the interface displacement followed by the main pulse of the soliton in the transition zone [15], [20] and reduce the soliton phase speed [14], [21].

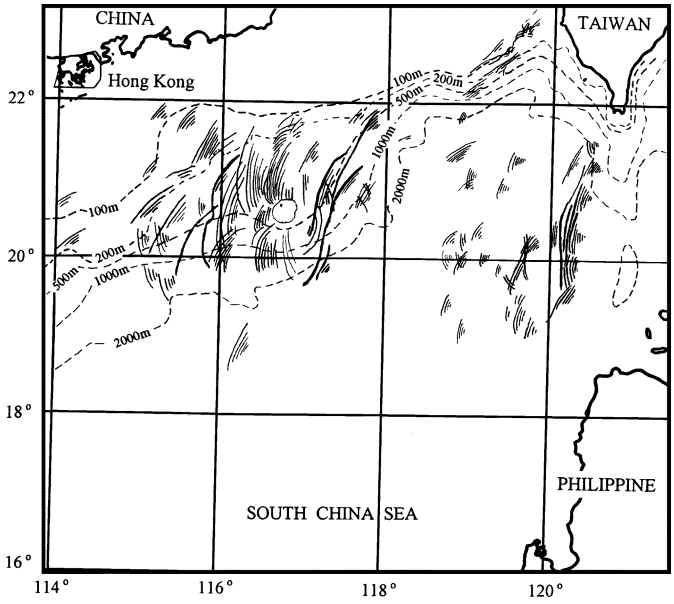

Fig. 1. Summary of the internal wave distributions in the northern SCS based on the available SAR imagery (from [24]).

With the exceptions described before, shoaling would induce a large-amplitude internal soliton breaking in the continental slope. Vlasenko and Hutter [22] used a numerical simulation to study the process of the internal soliton breaking on the continental slope. Their results showed that the internal soliton displayed some special characteristics in the current field when the wave was close to breaking. These characteristics included the soliton waveform becoming asymmetric and the time evolution of current velocity around the nodal point deformed, relative to the velocity in the uppermost and lowermost layers.

In the northern South China Sea (SCS), satellite images show that internal solitons are active [2], [13], [23], [24]. Both Ebbsemeyer *et al.* [24] and Bole *et al.* [2] found that internal solitons in the northern SCS occurred at the semidiurnal tidal frequency. They inferred that the internal soliton was generated by a point source in the Luzon Strait. Hsu *et al.* [25] studied historical synthetic aperture radar (SAR) images and found that the internal solitons were normally active in two regions: west of the Luzon Strait and in the continental slope of northern SCS (Fig. 1). Using the SAR images and a numerical model, Liu *et al.* [13] found the internal soliton west of Luzon Strait propagates westward, the length of the wave crest is approximately 200 km, and the vertical displacement of the isopycnals is approximately 100 m. This estimated displacement is much larger than the observations in the Andaman Sea [26], Sulu Sea [27], Georges Bank [28], Mid-Atlantic Bight [3], and the warm pool of the western equatorial Pacific [29].

However, theories and models of active solitons in the northern SCS need ground truth for validation. Field measurements, conducted as pilot studies for the Asian Seas International Acoustics Experiment (ASIAEX), were acquired during April of 1999 and 2000. Current velocity and temperature measurements from moorings are presented, analyzed, and discussed in this paper. The results not only provide ground truth for satellite images, but also provide validation for the earlier theoretical studies on the evolution and transformation of internal solitons.

V. Discussion and Summary

For the second and third types of soliton, the phenomena of the asymmetry of the soliton form and the complexity of the time evolution of U at mid-depths indicate that the soliton could reach the wave-breaking stage [22]. Two methods were applied to examine the wave-breaking stage; one is by examination of the ratio of the leading soliton amplitude $(\eta_{0,1})$ to h_2. Here, h_2 is defined as the water thickness below the nodal point. When h_2 is only around a factor 2 or 3 times $\eta_{0,1}$, the soliton is going to break [34], [35]. The second type of soliton, presented in Section III, had values for $\eta_{0,1}$ and h_2 of 90 ± 15 and 276 m, respectively. The value of $h_2/\eta_{0,1}$ is 3.18 ± 0.70. This result suggests that the soliton is close to or even on the breaking stage. Furthermore, the value of $h_2/\eta_{0,1}$ also suggests near overturning [22].

Another method for checking the soliton-breaking stage is to compare the maximum particle velocity $(u_{\max})$ and phase speed (c). When $u_{\max} > c$ in a two-layer fluid [36] or $u_{\max} > 0.8c$ in a continuous stratification fluid [37], the soliton would break. Most of the second types of leading soliton had $u_{\max}$ near or even larger than the estimated nonlinear phase speed and the soliton is near or even on the breaking stage. It is a reasonable hypothesis that the third type of soliton could have larger $u_{\max}$ than the second type of soliton, because the former induced a much larger temperature fluctuation. The observed third type of soliton could then be in the process of breaking.

The diurnal and semidiurnal tidal ellipses in 1999 and 2000 are shown as a function of depth in Fig. 14. During both years, the diurnal tide appeared to be more barotropic than the semidiurnal tide. The semidiurnal tide had a nodal point near 150 m during 1999 and was more rectilinear near mid-depth during 2000. To further evaluate the barotropic and baroclinic tidal current energies, band-pass filters were applied to obtain semidiurnal and diurnal current velocity time series at each depth. The frequency bandwidth was 0.008 c/h and was centered upon the K_1 and M_2 tidal frequencies for the diurnal and semidiurnal tides, respectively. These current velocity time series were then projected onto the barotropic and three baroclinic modes ($F_n(z)$, where n =0, 1, 2, and 3) by minimizing the mean-squared error between the band-passed current velocity and a linear combination of the modes. Finally, the variances of four modes were computed from the resulting projection time series [38]. The diurnal tidal variance was distributed over several modes with the largest percent of variance in the barotropic mode (Table II). The semidiurnal tidal variance was concentrated in the first baroclinic mode, which contained 69.8% and 86.9% of the variance during 1999 and 2000, respectively (Table II). More first baroclinic mode energy was, therefore, available to be transferred to the soliton from the semidiurnal tide than from the diurnal tide. This result could explain the observed semidiurnal occurrence of the solitons.